Thermal Modeling of NiMH Battery Powering Electric Vehicles

H. NESREDDINE and S. GUNTHER
Laboratoire des technologies de l'énergie (LTE)
Hydro-Quebec
600 Avenue Montagne, Shawinigan (QC) G9N 7N5
Canada

Abstract: - The aim of this study is to model the thermal behavior of NiMH batteries powering electric vehicles. Both the thermal and the hydrodynamic fields in the battery compartments are predicted using CFD simulations. The model developed switches between laminar free convection and turbulent mixed convection according to the fans state of operation. Simulations are carried out for the discharge phase of the battery (i.e. vehicle run phase) by setting the ambient temperature to 20 ^{o}C. The study put an emphasis on the validation of the model by comparing the numerical results to the experimental data collected during tests performed on an electric vehicle in an environmental chamber. Results reveal that evolutions of the predicted temperatures in both front and rear battery pack compartments are in accordance with the corresponding experimental data.

Key-Words: - NiMH battery, thermal management, thermal analysis, electric vehicle.

1 Introduction

The performance, life-cycle costs and safety issues of Nickel Metal Hydride (NiMH) batteries powering electric vehicles are very sensitive to the operating temperature. In hot or cold climates, batteries operation is compromised if they are not kept within an optimum range of temperature. For example, the desired operating temperature for a lead acid battery is 25 ^{o}C to 45 ^{o}C while the desired range for lithium-ion is between 20 ^{o}C and 40 ^{o}C [1]. It is important to regulate the operating temperature because it controls the electrochemical performance of the battery. Therefore, a well designed system is needed to create the necessary running conditions to avoid the battery exposure to high temperature and side effects such as premature aging and accelerated capacity-fade.

The present study is regarded as a first step towards an optimal design of the battery pack compartments. It will focus on the thermal modeling of the system rather than the study of parameter effects.

A commercial CFD software known as CFX4 is used to predict velocity and temperature distributions inside both battery compartments (front and rear) in order to detect any potential hot spots within the battery core. A special attention will be paid to the accuracy of the results supplied by the model. Hence, an exhaustive validation of the model will be performed by comparing the numerical results to the experimental data collected in a previous study [2].

2 Geometry and numerical resolution

2.1 Geometry description

The problem considered in this study consists of a system of two battery compartments containing identical batteries: 6 batteries in the front and 9 batteries in the rear. Each compartment is equipped with two identical fans which drive mechanically the cooling air by creating a vacuum. The inlets are constituted by many holes located at the bottom of each compartment. The cooling air flows through spaces that separate the batteries from each other and from the walls. Also, a plenum is managed under the batteries to assure flow uniformity. The geometric dimensions are summarized in table 1.

Description	length X	Height Y	Width Z
Front box	0.425 m	0.27 m	0.315 m
Rear box	0.3675 m	0.27 m	0.6375 m
Battery	0.415 m	0.2255 m	0.095 m
Outlet	0.154x0.0485 m^2		
Inlet	0.000961 m^2		
Air space	battery to battery: 0.0095m plenum: 0.01m battery to wall: 0.005 m		

Table 1 Physical dimensions of compartments.

In order to minimize the computer time and the memory required to run the model, we assume that the problem is symmetric. Therefore, the geometry has been created on half of both compartments in Cartesian coordinates system as displayed on figures 1 and 2. The symmetry plane coincides with the middle axis of the vehicle.
The front box is represented by a single block regrouping three batteries (numbered 1 through 3) while the rear box is constituted by two glued blocks: the first block contains three batteries and half (numbered 10 through 13) and the second block regroups two halves of two batteries (numbered 14 through 15). On the other hand, only one fan is represented in the geometry for both compartments according to the symmetry assumption.

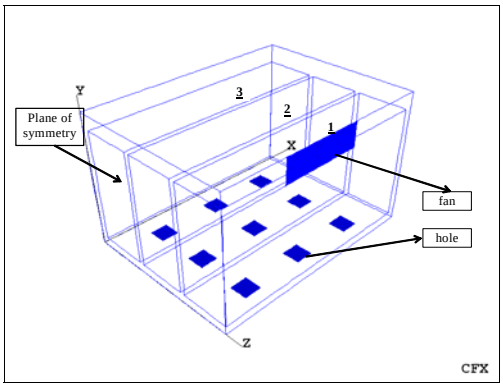

Fig. 1 Front battery pack compartment.

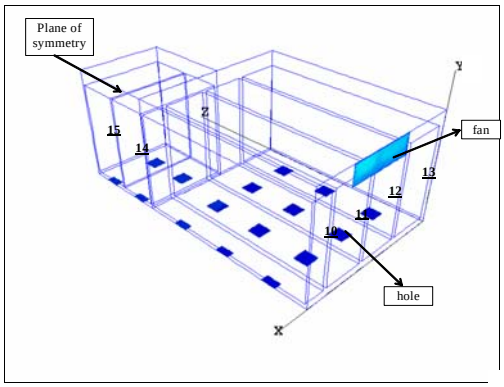

Fig. 2 Rear battery pack compartment.

2.2 Numerical procedure

The prediction of the temperature and the velocity fields for the problem under consideration is achieved by combining the laminar and turbulent convection models. Default turbulence coefficients were assumed [3].
The laminar free convection model is used when the fans are not functioning while the standard k-ε model with mixed convection heat transfer allows to model turbulence effects when the fans are running. A logarithmic wall function is used to count for laminarization of the flow in the wall vicinity.

The following assumptions have been adopted in order to limit the complexity of the numerical resolution:

- heat generation is uniformly distributed across each battery and depends only on the current.
- both compartments are not insulated and are fully surrounded by still air at a uniform ambient temperature.
- the flow is laminar and only natural convection heat transfer regime prevails when the fans are not functioning (Off position).
- the flow is turbulent and both natural and forced convection are considered when the fans are running (On position).
- the air flow through holes when the fans are not functioning is negligible.
- the effects of the acceleration, the deceleration and the speed of the vehicle during the running phase are ignored.

The batteries are considered as a solid material having the physical properties listed in table 2.

Density [kg/m^3]	Specific heat [J/kg.°C]	Thermal conductivity [W/m.°C]
1600	900	0.585

Table 2 Physical properties of NiMH battery [4].

Concerning the boundary conditions, the ambient temperature is imposed at the inlets (holes) and on the wall constituting the faces of the battery compartment. Furthermore, the mass flow of air in the front and the rear are fixed to 120m^3/hr and 180m^3/hr, respectively.
The time dependant heat generation within the battery has been computed as a volumetric heat generation rate [W/m^3] in the solid energy equation as follows:

$$Q(t) = \frac{R.I^2(t)}{V} \quad (1)$$

where
R resistance of the battery [Ω]
I(t) current crossing the battery [Amps]
V volume of the battery [m^3]

It is important to mention that the current I(t) is a function of time as dispatched on figure 3. This figure represents current data at 5 seconds interval.
Under the above assumptions, the governing equations have been solved simultaneously under transient conditions for both compartments.

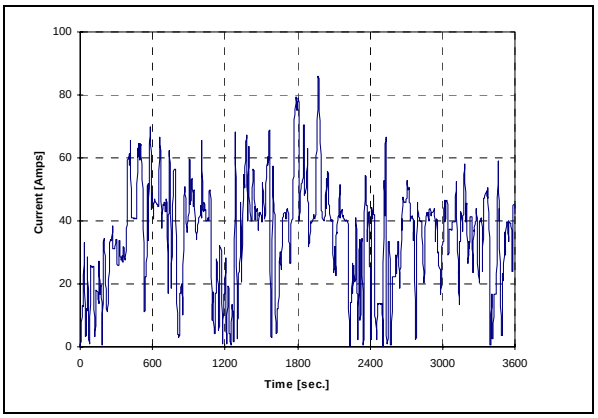

Fig. 3 Current profile during discharge phase.

3 Results and discussion

The results obtained from the simulations will be presented in the form of temperature and velocity fields at the end of each run (after 60 minutes) at different planes. The results include also the prediction of the transient temperature evolution at the sensors locations in both compartments. These temperature profiles are compared to the corresponding experimental data for the validation purpose of the model.

3.1 Transient temperature profiles

The comparison of the predicted temperature evolution with the experimental data collected at the sensor located on battery #2 (front box) is displayed on figure 4. A good agreement is obtained between numerical and experimental results regardless the fans' On-Off state. In fact, the model predicts accurately the temperature fluctuations in the box. The average relative error is approximately 0.2% based on the Kelvin absolute temperature scale.
Concerning the rear box, the comparison between the predicted and the measured temperature at the sensors located on the terminals of batteries #11 and #14 are displayed on figures 5 and 6 respectively. The examination of these two figures shows that the predictions are in accordance with the experimental data. The average error is 0.19% for the left side (battery #11) and 0.12% for the right side (battery #14).
As the batteries are discharging, the temperature in both compartments is increasing due to Joule effects. After, approximately 33 minutes, the recorded temperature reaches the set-point temperature of the controller which activates the fans in order to lower the temperature inside the compartments by evacuating the heat outside.

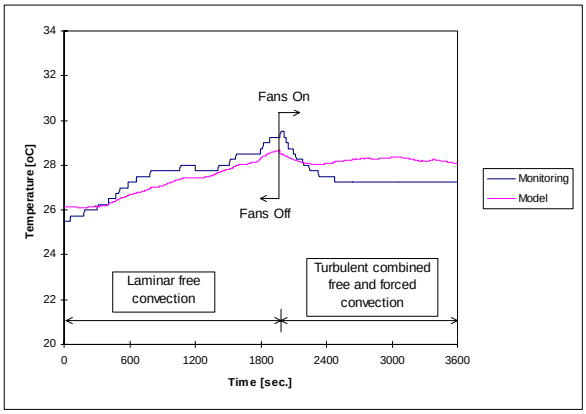

Fig. 4 Temperature evolution in terminal 2.

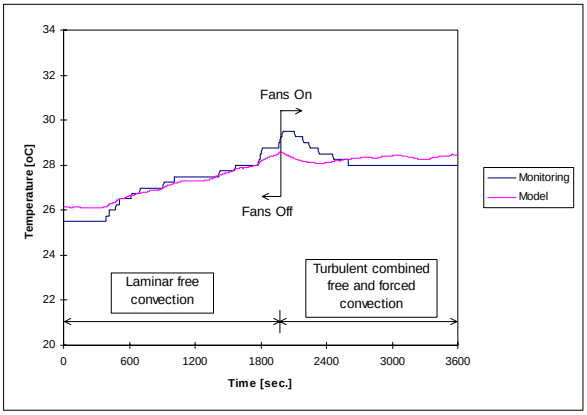

Fig. 5 Temperature evolution in terminal 11.

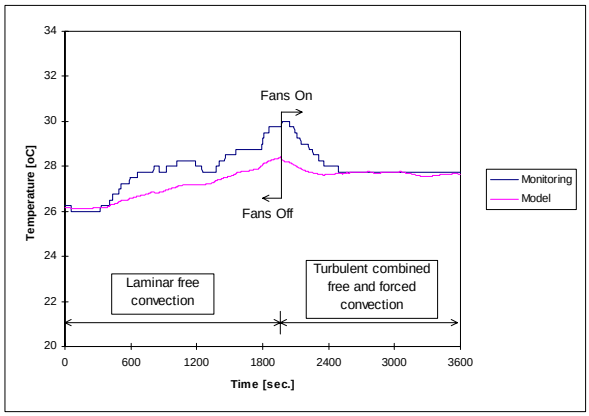

Fig. 6 Temperature evolution in terminal 14.

3.2 Temperature and velocity distributions

The front compartment is taken as example to present the temperature and the velocity distributions obtained at different planes after an hour of running [5].

The examination of the results concerning the front box reveals that the hottest region in the box is located in the core of battery # 2. Even though the fans are running, the corresponding temperature is as high as 303 K (30°C). It is interesting to mention here that the temperature at the location of the sensor is lower than that at the center of the battery; the difference is approximately 2°C.

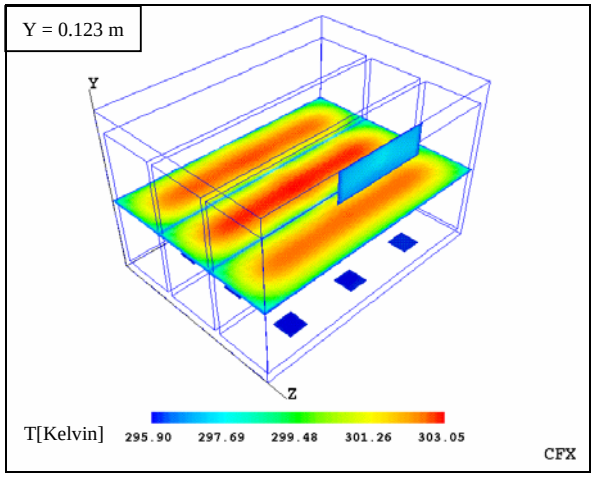

Fig. 7 Front compartment temperature distribution.

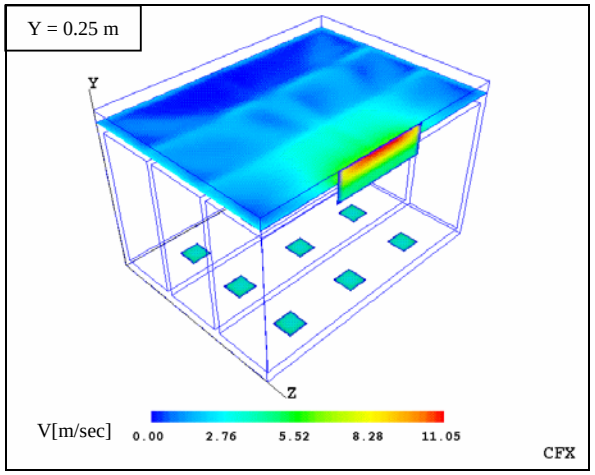

Fig. 8 Front compartment velocity distribution.

Concerning the velocity distribution, the air movement underneath the batteries seems to be quasi uniform because of the existence of the plenum. Similarly, the flow between the batteries is quite homogeneous except maybe for the air space at the front face of the box (between battery #3 and the wall) where the velocity is less important than elsewhere. On the other hand, the mass of air on the top of the battery #3 seems to be still. The reason is associated to the vortex (flow recirculation) created by ascendant and descendant flows. This phenomenon is not observed for the other batteries since they are relatively closer to the fan which extracts the air out of the box, hence, eliminating any possibility of vortex development.

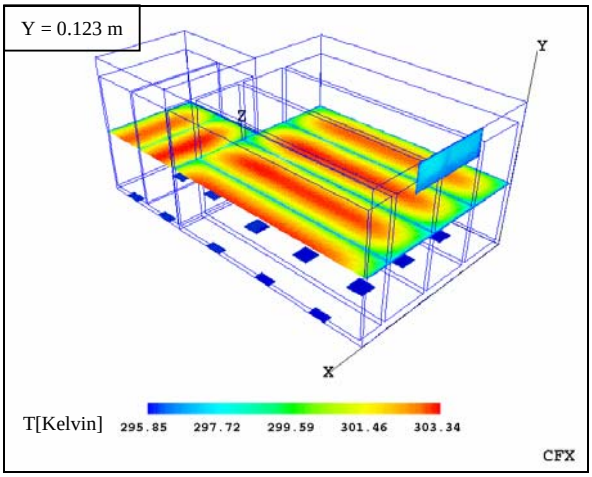

Fig. 9 Rear compartment temperature distribution.

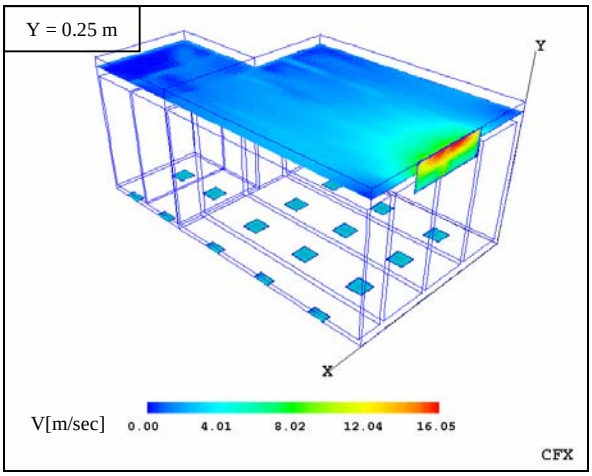

Fig. 10 Rear compartment velocity distribution.

Concerning the rear box, the hottest batteries are those located at the center (#10, #11, #12 and #14) but the most critical one seems to be the last one, say the battery #14. This can be explained by the poor air circulation on the back side of this specific battery as shown by the velocity and vector fields. In this particular region, the fan is relatively far which favors free convection forces to drive the cooling air by means of temperature (or density) gradients. It should be mentioned here that the heat transfer deteriorates when the convection

mechanism changes from forced to free regime. Consequently, the temperature arises rapidly as the heat removal decreases.

4 Conclusions

The thermal performance of NiMH batteries powering electric vehicle has been numerically investigated for the running phase.
Results have shown that the hottest batteries are those located in the center of the compartments where the temperature can be as high as 30 ^{o}C for a surrounding temperature of 20 ^{o}C.
The model developed on CFX platform is reliable for temperature and velocity prediction. This tool can be used for the optimization of the algorithm implemented in the controller for thermal management purpose. In addition, it is helpful for battery stacking and spacing as well as pressure drop and fan parasitic power requirements.
It can also be used for the study of the effects of some parameters such as the insulation and the air mass flow especially during the cold temperature conditions and recharging phase of the batteries.

References:

[1] Pesaran, A. A., Burch, S. and Keyser, M., *An Approach for Designing Thermal Management Systems for Electric and Hydrid Vehicle Battery Packs*, Report NREL/CP-540-25992, 1999.

[2] Jean-François Morneau, *Evaluation of cold temperature performance of a NIMH battery powered E.V*, LTE Report RT-0068/1998.

[3] CFX 4.2 Flow solver user guide. AEA Technologies

[4] Craig Blazakis, *Electric vehicle battery box thermal analysis*, Report of PDC (product design center), 1997.

[5] Hakim Nesreddine, *Thermal modeling of NIMH battery*, LTE Report RT-0132/1999.